Theoretical Characterization of the Reaction

$CH_3 + OH \rightarrow CH_3OH \rightarrow$ products :

The $^1CH_2 + H_2O$, $H_2 + HCOH$, and $H_2 + H_2CO$ Channels

Stephen P. Walch[a]
ELORET Institute
Palo Alto, Ca. 94303

Abstract. The potential energy surface (PES) for the CH_3OH system has been characterized for the $^1CH_2 + H_2O$, $H_2 + HCOH$, and $H_2 + H_2CO$ product channels using complete-active-space self-consistent-field (CASSCF) gradient calculations to determine the stationary point geometries and frequencies followed by CASSCF/ internally contracted configuration-interaction (CCI) calculations to refine the energetics. The $^1CH_2 + H_2O$ channel is found to have no barrier. The long range interaction is dominated by the dipole-dipole term, which orients the respective dipole moments parallel to each other but pointing in opposite directions. At shorter separations there is a dative bond structure in which a water lone pair donates into the empty a'' orbital of CH_2. Subsequent insertion of CH_2 into an OH bond of water involves a non-least-motion pathway. The $H_2 + HCOH$, and $H_2 + H_2CO$ pathways have barriers located at -5.2 kcal/mol and 1.7 kcal/mol, respectively, with respect to $CH_3 + OH$. From comparison of the computed energetics of the reactants and products to known thermochemical data it is estimated that the computed PES is accurate to $\pm$ 2 kcal/mol.

[a]Mailing Address: NASA Ames Research Center, Moffett Field, CA 94035.

I. Introduction

The CH_3 + OH reaction has at least six possible product channels:

$$CH_3 + OH + M \rightarrow CH_3OH + M \qquad (1a)$$

$$CH_3 + OH \rightarrow CH_2OH + H \qquad (1b)$$

$$CH_3 + OH \rightarrow CH_3O + H \qquad (1c)$$

$$CH_3 + OH \rightarrow {}^1CH_2 + H_2O \qquad (1d)$$

$$CH_3 + OH \rightarrow HCOH + H_2 \qquad (1e)$$

$$CH_3 + OH \rightarrow H_2CO + H_2 \qquad (1f)$$

The role of reaction 1d has been controversial. The room temperature rate for the reverse of reaction 1d has been measured by Hatakeyama et al. [1] as $\approx 3 \times 10^{-12}$ cm^3 molecule^{-1}cm^{-1}, while Hack et al. [2] obtained 3.5×10^{-11} cm^3 molecule^{-1}cm^{-1}, or about an order of magnitude faster. The latter rate is approximately gas kinetic and implies no barrier. Using currently accepted heats of formation [3], and a singlet-triplet splitting for methylene of 9 kcal/mol, reaction 1d is exothermic by 0.7 kcal/mol at 0K. Thus, the forward reaction is also expected to be very fast.

Dean and Westmoreland [4] have used a variant of Rice-Ramsperger-Kassel-Marcus (RRKM) theory called QRRK theory to model the product distributions in the CH_3 + OH reaction. In this work the parameters for 1b and 1c were based on estimated rates for the reverse reaction. The parameters for reaction 1f were taken from calculations [5] and the rate for reaction 1d was taken from Ref. 1. According to these studies, at room temperature and moderate pressure CH_3OH is the dominant product, while at flame temperatures reaction 1b is thought to take

over. The HCOH + H_2 channel does not appear to have been considered in these studies, though theory [5] indicates essentially no barrier with respect to CH_3 + OH. This study indicated that production of $^1CH_2$ (reaction 1d) is a minor channel. By contrast a model proposed by Pilling and coworkers [6] which makes use of the rate for the reverse of reaction 1d due to Hack et al. [2] indicates that reaction 1d is the dominant channel above room temperature.

Recently Smith [7] has also reported RRKM calculations for CH_3 + OH. These calculations as well as the work of Pilling et al. [6] have indicated a need for more accurate potential energy surface (PES) information for the $^1CH_2$ + H_2O, H_2 + HCOH, and H_2 + H_2CO product channels. The most accurate previous theoretical study of these channels in the CH_3OH system was carried out by Harding, Schlegal, Krishnan, and Pople [5] using Møller-Plesset perturbation theory with a 6-311G** basis set. Although these calculations were carefully carried out, there is probably considerable uncertainty in the energetics; by current standards, both the basis set and treatment of electron correlation can be improved upon. More recently the bond dissociation energies of CH_3OH have been computed by Bauschlicher, Langhoff, and Walch [8] using the modified coupled-pair functional method. Similar calculations were carried out by Pople and co-workers [9] using the G2 method, which includes some empirical corrections. These calculations accurately determined the heats of formation of the CH_3O and CH_2OH species, but they did not consider the portions of the PES leading to the $^1CH_2$ + H_2O, H_2 + HCOH, and H_2 + H_2CO product channels. Thus, these regions of the PES are reexamined here.

Qualitative features of the potential energy surfaces are discussed in Sec. II, the computational method is discussed in Sec. III, the results are presented in Sec. IV, and the conclusions are given in Sec. V.

II. Qualitative Features.

CH_2 has two low-lying states. The $^3B_1$ ground state which will be drawn as:

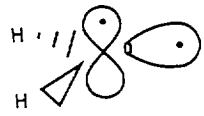

has two orthogonal high-spin coupled singly occupied orbitals, while the $^1A_1$ state, which is ≈ 9 kcal/mol higher, is drawn as:

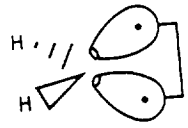

i.e., the two orbitals corresponding to the C lone pair are singlet paired. If these orbitals are solved for self consistently in a generalized valence bond wavefunction [10] the overlap integral between them is ≈ 0.7. Thus, the singlet state of CH_2 may be characterized as a singlet biradical, but the orbitals of the lone pair have a substantial overlap, which must be maintained while inserting into a single bond if the process is to occur without a substantial barrier. In terms of multiconfigurational self-consistent-field (MCSCF) theory, the biradical character in CH_2 arises because of a near degeneracy effect between an sp hybrid lone pair and an empty 2p-like a'' orbital.

The insertion of $^1CH_2$ into a bond pair occurs via a non-least-motion pathway. This process is completely analagous to the non-least-motion addition of the $^2\Pi$

state of CH to H_2, as discussed by Dunning and Harding [10]. In that case the CH and H_2 approach each other with the bond axes parallel and for this orientation the C lone pair and H_2 bond pair orbitals are able to evolve into two CH bonding orbitals without breaking either bond. These orbital changes are consistent with the orbital phase continuity principle arguments made by Goddard [11].

In the case of $^1CH_2 + H_2O$ the long range interaction is dominated by the dipole-dipole term, which leads to an initial approach with the dipoles parallel to each other but pointed in the opposite direction. At shorter separation there is a dative bonded structure where one lone pair on H_2O donates into the empty C 2p-like orbital of CH_2. This structure is a minimum on the PES. Insertion of CH_2 into one of the H_2O bonds requires rotating H_2O such that one OH bond is in the plane defined by O and the bisector of $\angle$ HCH. This orientation is similar to the orientation favored for non-least-motion insertion of CH into H_2.

Insertion of $^1CH_2$ into H_2O involves very little barrier. The insertion of hydroxy methylene (HCOH) into H_2, however, is found to exhibit a barrier of 13.9 kcal/mol. The lower reactivity of HCOH as compared to CH_2 results from delocalization of an O lone pair into the empty C 2p orbital. The resultant exclusion effect reduces the 2s $\rightarrow$ 2p near-degeneracy effect and thus results in less biradical character in the substituted carbene.

III. Computational Details.

Two different basis sets were used in this work. For the CASSCF gradient calculations the polarized double-zeta set of Dunning and Hay [12] was used. The basis set for C and O is a (9s5p)/[3s2p] basis augmented by a single set of 3d functions with exponents of 0.75 and 0.85 for C and O, respectively. The H basis is (4s)/[2s] augmented with a single set of 2p functions with exponent 1.00. The basis set used in the CI calculations is the Dunning correlation consistent triple-zeta double-

polarization basis set [13]. This basis is [4s3p2d1f] for C and O and [3s2p1d] for H and is described in detail in Ref. 13.

In the CASSCF calculations the electrons in the bonds which are being made or broken were included in the active space. In the case of the $^1CH_2 + H_2O$ and $H_2CO + H_2$ channels, there were six active electrons and six active orbitals. The correlated electrons correspond to the CO bond, the OH bond, and one CH bond of CH_3OH and evolve to the C lone pair of CH_2 and the two OH bond pairs in the case of $^1CH_2 + H_2O$ and the CO σ and π bonds and the H_2 bond in the case of $H_2CO + H_2$. The remaining 12 electrons are inactive in the CASSCF calculation. In the case of the $HCOH + H_2$ channel, there were four active electrons and four active orbitals. The correlated electrons correspond to two CH bonds in CH_3OH and to the C lone pair in HCOH and the H_2 bond pair in the $HCOH + H_2$ limit. The remaining 14 electrons were inactive in the CASSCF calculation. In generating the set of reference configurations, no more than two electrons were permitted in the weakly occupied CASSCF orbitals. All but the O 1s and C 1s electrons were correlated in the CCI calculations.

The CASSCF/gradient calculations used the SIRIUS/ABACUS system of programs [14], while the CCI calculations were carried out with MOLPRO [15,16]. Most of the calculations were carried out on the NASA Ames Cray Y-MP; although some of the CCI calculations were carried out on the NAS facility Y-MP.

IV. Discussion.

Table I shows computed energetics for the portions of the CH_3OH surface which were considered in this work. The computed energetics were obtained from the CCI energies (including the multireference analogue of the Davidson correction [17]) plus the zero-point energies from the CASSCF calculations. (See Tables IIa-IIc.) Thus, these energetics should be compared to experimental values at 0 K. The computed

frequencies and rotational constants for the saddle points for $CH_2O + H_2$, HCOH + H_2, and $^1CH_2 + H_2O$, (denoted as CH_2O-H_2, HCOH-H_2, and CH_2-H_2O, respectively) and for the $CH_2 + H_2O$ dative bonded structure (denoted as $CH_2.H_2O$) are also given in Table III. The stationary point corresponding to $CH_2.H_2O$ is a minimum on the PES, but there is one very small frequency (26 cm^{-1}), which corresponds to a hindered rotation of the CH_2 and H_2O with respect to each other.

The computed energy separations discussed here, in each case, involve breaking two bonds and forming two new bonds; thus, the errors in the individual bond strengths cancel and the computed energetics are expected to be accurate. However, in Ref. 2 it was shown that, for calculations of about the same quality as reported here, the error in the C-O bond strength in CH_3OH is 6.5 kcal/mol. Thus, in order to compute energies with respect to $CH_3 + OH$, the experimental 0 K value of 90.2 kcal/mol [18] was used for the C-O bond strength. The locations of the H + CH_3O and H + CH_2OH asymptotes were taken as the best-estimate values from Ref. 2. This places H + CH_3O and H + CH_2OH at 14.8 kcal/mol and 6.0 kcal/mol above $CH_3 + OH$, respectively. The experimental locations of $^1CH_2 + H_2O$ and CH_2O + H_2 with respect to CH_3OH were derived from the JANAF [3] heats of formation of H_2, CH_2O, CH_3, OH, H_2O(g), and $^3CH_2$, plus a singlet-triplet splitting in CH_2 of 9.0 kcal/mol and the value for the C-O bond strength in CH_3OH given above.

From Table I it is seen that the computed $CH_3OH \rightarrow {}^1CH_2 + H_2O$ separation is 0.7 kcal/mol smaller than experiment, while the computed $CH_3OH \rightarrow CH_2O$ + H_2 separation is 0.6 kcal/mol smaller than experiment. It is also seen that the computed results of Harding et al. [5] are 5.4 kcal/mol larger and 2.3 kcal/mol smaller, respectively, for the same separations. The computed barrier heights for $CH_3OH \rightarrow HCOH + H_2$ and $CH_3OH \rightarrow CH_2O + H_2$ obtained in Ref. 5 are 6.0 kcal/mol and 4.6 kcal/mol larger than the barrier heights obtained in the present

work. These differences presumably reflect a combination of the larger basis set and more extensive correlation treatment in the present calculations. Based on the comparison to experiment for the $^1CH_2 + H_2O$ and $CH_2O + H_2$ asymptotes it is reasonable to assign error bars of $\approx \pm$ 2 kcal/mol to the computed energetics in this work.

The computed energetics for the CH_3OH system are also shown schematically in Fig. 1. From Fig. 1 it is seen that only the $CH_2O + H_2$ channel exhibits a barrier (1.7 kcal/mol.) with respect to $CH_3 + OH$. The $H_2 + HCOH$ channel has a barrier, but it is below $CH_3 + OH$. The $^1CH_2 + H_2O$ channel has no barrier and is computed to be 1.4 kcal/mol below $CH_3 + OH$. The $CH_3O + H$ and $CH_2OH + H$ channels are endoergic with respect to $CH_3 + OH$, but no intermediate barriers are expected. Thus, from this work the $^1CH_2 + H_2O$, $HCOH + H_2$, and $CH_2O + H_2$ channels are all found to be accessible from $CH_3 + OH$.

Fig. 2 shows the energy as a function of r_{CO} for the addition of $^1CH_2$ to H_2O, while the computed energies are given in Table IV. Two stationary points have been located along this minimum energy path. At long r_{CO} the dominant interaction is dipole-dipole, which results in an orientation with the dipole moments of the approaching molecules parallel to each other but pointing in opposite directions, as illustrated in Fig. 2. At shorter r_{CO} there is a minimum on the PES with C_s symmetry, followed by a saddle point with no symmetry for insertion of $^1CH_2$ into an OH bond of water. In order to characterize the minimum energy path, a gradient calculation was carried out starting at the saddle point and proceeding toward the minimum. CCI calculations were then carried out at the geometries corresponding to each step on the walk. This calculation defines the minimum energy path between the saddle point and minimum. It is not possible to do the same calculation for the portion of the PES connecting the minimum and the $^1CH_2$

+ H_2O asymptote, since there is no well-defined way to follow the gradient uphill. In order to characterize this portion of the PES, calculations were carried out with the CH_2 and H_2O molecules fixed at their equilibrium geometries and oriented with the planes of the molecule parallel to each other and the CO bond perpendicular to both molecular planes in the orientation shown in Fig. 2. For this geometric orientation, r_{CO} was varied and the resulting energies at the CCI level are also included in Fig. 2.

The main features of Fig. 2 are a shallow minimum followed by a small barrier to formation of CH_3OH. However, the barrier is below the $^1CH_2$ + H_2O asymptote and therefore the bottleneck on the vibrationally adiabatic curve is expected to occur in the entrance channel region. The main feature responsible for the entrance channel bottleneck is the building in of bending modes, which arise from electrostatic (dipole-dipole, dipole-quadrapole, and quadrapole-quadrapole) interactions. In order to define this interaction, dipole and quadrapole moments (about the center of mass) were computed for $^1CH_2$ and H_2O and are given in Table V. The experimental values [19] for H_2O (in a.u.) are μ = 0.73, Q_{xx} = 1.955, Q_{yy} = -1.859, and Q_{zz} = -0.097; which are in reasonable agreement with the computed values.

V. Conclusions.

The potential energy surface (PES) for the CH_3OH system has been characterized for the $^1CH_2$ + H_2O, H_2 + HCOH, and H_2 + H_2CO product channels using complete-active-space self-consistent field (CASSCF) gradient calculations to determine the stationary point geometries and frequencies followed by CASSCF/ internally contracted configuration-interaction (CCI) calculations to refine the energetics.

The H_2 + H_2CO, and H_2 + HCOH pathways have barriers located at 1.7 kcal/mol and - 5.2 kcal/mol with respect to CH_3 + OH. The $^1CH_2$ + H_2O channel is found to

have no barrier in the absence of vibrational zero-point effects. However, the long range-interaction is dominated by a dipole-dipole term and the zero-point effects due to this interaction are expected to lead to a bottleneck on the vibrationally adiabatic minimum energy path. The $^1CH_2 + H_2O$ asymptote is computed to be 1.4 kcal/mol below $CH_3 + OH$. Thus, all three of these channels are expected to be accessible at moderate temperatures.

From comparison of the computed energetics of the reactants and products to known thermochemistry it is estimated that the computed PES is accurate to $\pm$ 2 kcal/mol.

Acknowledgement. SPW was supported by NASA cooperative agreement number NCC2-478.

References

1. S. Hatakeyama, H. Bandow, M. Okuda, and H. Akimoto, J. Phys. Chem., **85**, 2249(1981).
2. W. Hack, H.Gg. Wagner, and A. Wilms, Ber. Bunsen-Ges. Phys. Chem. **92**, 620(1988).
3. M.W. Chase, Jr.,C.A. Davies, J.R.Downey, Jr., D.J. Frurip, A.A. McDonald, and A.N. Syverud, J. Phys. Chem. Ref. Data, **14**, Suppl. 1(1985).
4. A.M. Dean and P.R. Westmoreland, Int. J. Chem. Kinet., **19**, 207(1987).
5. L.B. Harding, H.B. Schlegal, R. Krishnan, and J.A. Pople, J. Phys. Chem., **84**, 3394(1980).
6. N.J. Green, A.R. Pereira, M.J. Pilling, and S.H. Robinson, presented at the 23rd Symposium (International) on Combustion, 1990; poster.
7. G.P. Smith, 203rd ACS National Meeting, San Francisco, April 1992.
8. C.W. Bauschlicher, Jr., S.R. Langhoff, and S.P. Walch, J. Chem. Phys., **96**, 450(1991).
9. L.A. Curtiss, L.D. Kock, and J.A. Pople, J. Chem. Phys., **95**, 4040(1991).
10. T.H. Dunning Jr. and L.B. Harding, Theory of Chemical Reaction Dynamics, M. Baer ed, CRC Press, Boca Raton, Florida, 1985, pp. 1-69.
11. W.A. Goddard III, J. Amer. Chem. Soc., **94**, 793(1972).
12. T.H. Dunning,Jr and P.J. Hay in Methods of Electronic Structure Theory, H.F. Schaefer III ed., Plenum Publishing, 1977
13. T.H. Dunning Jr., J. Chem. Phys., **90**, 1007(1989).
14. SIRIUS is an MCSCF program written by H.J. Jensen and H. Agren and ABACUS is an MCSCF derivatives program written by T. Helgaker, H.J.

Jensen, P. Jørenson, J. Olsen, and P.R. Taylor.

15. H.-J. Werner and P.J. Knowles, J. Chem. Phys., **89**, 5803(1988).

16. P.J. Knowles and H.-J. Werner, Chem. Phys. Lett., **145**, 514(1988).

17. S.R. Langhoff and E.R. Davidson, Int. J. Quantum Chem,, **8**, 61(1974).

18. D.D. Wagman, W.H. Evans, V.B. Parker, S.H. Schumm, I. Halow, S.M. Bailey, K.L. Churney, and R.L. Nutall, J. Phys. Chem. Ref. Data, **11**, Suppl. 1(1982).

19. C.G. Gray and K.E. Gubbins, Theory of Molecular Fluids, Vol. I, Clarendon Press, Oxford (1984).

Table I. Computed Energetics for CH_3OH[a,b]

	calc.	exp(0K)	Harding et al.
$CH_3 + OH$		90.2	
$HCOH\text{-}H_2$	85.0		91.0
$HCOH + H_2$	71.1		71.1
$^1CH_2 + H_2O$	88.8	89.5[c]	94.9
$CH_2O\text{-}H_2$	91.9		96.5
$CH_2O + H_2$	18.1	18.7	16.4
CH_3OH	0.0	0.0	0.0

[a] CASSCF/CCI with a [4s3p2d1f/3s2p1d] basis set.

[b] Relative energies in kcal/mol (including zero-point energy).

[c] Using $^3CH_2 \rightarrow {}^1CH_2$ separation of 9.0 kcal/mol.

Table IIa. Computed energies and zero-point corrections.

$$CH_3OH \rightarrow CH_2O + H_2$$

	Energy[a]	zero-point energy[b]	Δ E[c]
CH_3OH	-115.51397(-.54566)	0.05258	0.0
CH_2O-H_2	-115.35603(-.39071)	0.04407	91.9
CH_2O+H_2	-115.47215(-.50189)	0.03768	18.1

[a] Energy in E_H. The first energy is the CCI energy, while the energy in parenthesis includes a multi-reference Davidson correction and is with respect to -115. E_H.

[b] zero-point energy in E_H.

[c] relative energy in kcal/mol including zero-point energy and a multi-reference Davidson's correction.

Table IIb. Computed energies and zero-point corrections.

$$CH_3OH \rightarrow^1 CH_2 + H_2O$$

	Energy[a]	zero-point energy[b]	Δ E[c]
CH_3OH	-115.51397(-.54566)	0.05258	0.0
CH_2-H_2O	-115.36931(-.40561)	0.04366	82.3
CH_2+H_2O	-115.35989(-.39040)	0.03884	88.8

[a] Energy in E_H. The first energy is the CCI energy, while the energy in parenthesis includes a multi-reference Davidson correction and is with respect to -115. E_H.

[b] zero-point energy in E_H.

[c] relative energy in kcal/mol including zero-point energy and a multi-reference Davidson's correction.

Table IIc. Computed energies and zero-point corrections.

$$CH_3OH \rightarrow HCOH + H_2$$

	Energy[a]	zero-point energy[b]	Δ E[c]
CH_3OH	-115.50589(-.54231)	0.05258	0.0
HCOH-H_2	-115.35803(-.39640)	0.04225	85.0
HCOH+H_2	-115.37823(-.41465)	0.03828	71.1

[a] Energy in E_H. The first energy is the CCI energy, while the energy in parenthesis includes a multi-reference Davidson correction and is with respect to -115. E_H.

[b] zero-point energy in E_H.

[c] relative energy in kcal/mol including zero-point energy and a multi-reference Davidson's correction.

Table III. Computed saddle point frequencies and rotational constants(cm^{-1}).

	CH_2O-H_2	HCOH-H_2	$CH_2.H_2O$	CH_2-H_2O
ω_1	3195	4130	3860	3723
ω_2	2295	3199	3744	3319
ω_3	1740	2323	3187	3222
ω_4	1574	1564	3113	2091
ω_5	1429	1498	1691	1560
ω_6	1369	1347	1515	1524
ω_7	916	1291	802	1119
ω_8	$2877i$	1122	610	949
ω_9	3278	934	337	703
ω_{10}	1273	622	334	438
ω_{11}	1211	513	161	387
ω_{12}	1065	$1414i$	26	$1850i$
A	3.345	3.042	4.117	4.640
B	0.944	0.839	0.358	0.496
C	0.863	0.764	0.349	0.478

Table IV. Computed energies and zero-point corrections[a].

$$CH_2 + H_2O \rightarrow CH_2 - H_2O$$

r_{CO}	CAS Energy	CI Energy[b]	zero-point energy	total[c]
3.834	-115.00924	-115.36931(-.40561)	0.04366	(-.36225)
3.929	-115.01305	-115.36889(-.40409)	0.04449	(-.35960)
4.076	-115.01765	-115.36968(-.40420)	0.04550	(-.35870)
4.207	-115.02142	-115.37055(-.40452)	0.04546	(-.35906)
4.310	-115.02426	-115.37130(-.40480)	0.04523	(-.35957)
4.386	-115.02635	-115.37189(-.40503)	0.04500	(-.36003)
4.437	-115.02785	-115.37230(-.40516)	0.04482	(-.36034)
4.471	-115.02890	-115.37254(-.40517)	0.04470	(-.36047)
4.528	-115.03024	-115.37237(-.40450)	0.04421	(-.36029)
5.0	-115.02970	-115.36971(-.40136)		
5.5	-115.02892	-115.36727(-.39843)		
6.0	-115.02797	-115.36541(-.39630)		
6.5	-115.02710	-115.36400(-.39475)		
7.0	-115.02635	-115.36294(-.39358)		
8.0	-115.02526	-115.36151(-.39206)		
9.0	-115.02464	-115.36076(-.39127)		
10.0	-115.02433	-115.36040(-.39091)		

[a] All energies in E_H. r_{CO} is in a. u.

[b] The first energy is the CCI energy, while the energy in parenthesis includes a multi-reference Davidson correction and is with respect to -115. E_H.

[c] Energy with respect to -115. E_H. The energy includes the zero-point correction and a multi-reference Davidson correction.

Table V. Computed dipole and quadrapole moments [a].

	μ	Q_{xx}	Q_{yy}	Q_{zz}
H_2O	0.768	-1.987	1.955	0.032
CH_2 $^1A_1$	0.679	1.187	0.496	-1.683

[a] Properties are in a.u. Quadrapole moment is with respect to the center of mass. The molecule is in the YZ plane with the C_2 axis in the Z direction.

Figure Captions.

Fig. 1. Schematic diagram of the potential energy surface for CH_3 + OH. The location of the CH_3 + OH asymptote with respect to CH_3OH is taken from experiment, while the locations of the CH_2OH + H aand CH_3O + H asymptotes are from previous calculations.

Fig. 2. The potential for $^1CH_2$ + H_2O from CCI calculations along the CASSCF minimum energy path. See the text.

Fig. 1

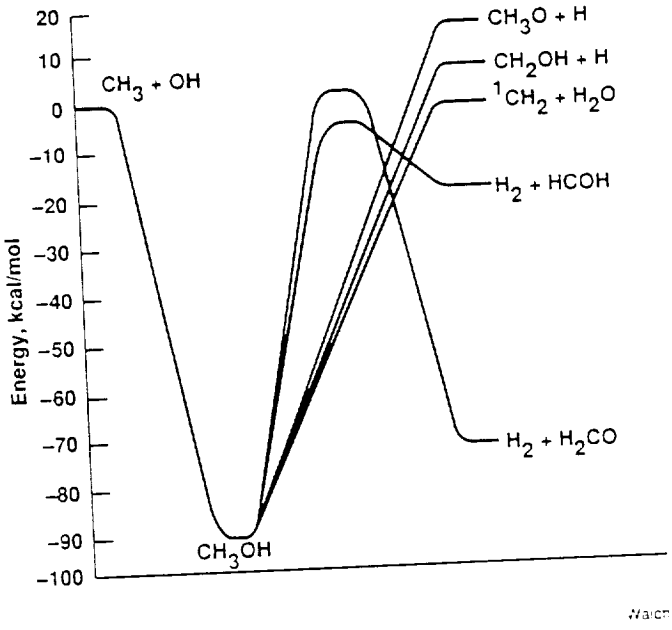
20
10
0
−10
−20
−30
−40
−50
−60
−70
−80
−90
−100
Energy, kcal/mol
$CH_3 + OH$
CH_3OH
$CH_3O + H$
$CH_2OH + H$
$^1CH_2 + H_2O$
$H_2 + HCOH$
$H_2 + H_2CO$

Walch

Fig. 2

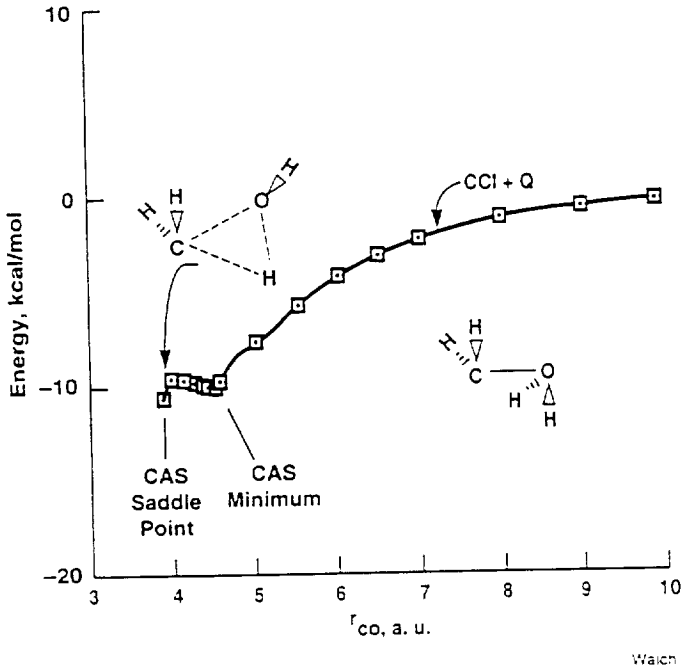
10
0
−10
−20
Energy, kcal/mol
3
4
5
6
7
8
9
10
r_{CO}, a. u.
CCl + Q
CAS
Saddle
Point
CAS
Minimum
H
C
O
H
H
C
O
H
H

Walch